ACS MATERIALS Au
AN OPEN ACCESS JOURNAL OF THE AMERICAN CHEMICAL SOCIETY

pubs.acs.org/materialsau

Perspective

Rationalization of Double Perovskite Oxides as Energy Materials: A Theoretical Insight from Electronic and Optical Properties

Manasa G. Basavarajappa and Sudip Chakraborty*

Cite This: *ACS Mater. Au* 2022, 2, 655−664

Read Online

ACCESS | Metrics & More | Article Recommendations

ABSTRACT: The quest for clean energy conversion has become one of the most important efforts for tackling the greenhouse effect for a sustainable environment. This involves energy-scavenging processes like photovoltaics and catalysis, which have been manifested using the solar spectrum. For high-efficiency and durable conversion processes, the search for the low-cost, stable, and environment-friendly functional materials is elusive. In the field of solar cells and catalysis, double perovskite oxides (DPOs) have emerged as potential candidates in recent years. Through compositional tuning and band gap engineering, a plethora of materials are being developed for pertinent applications in this field of energy. Oxide perovskites possess the advantage of a high carrier lifetime compared to that with halide perovskites, which can be beneficial for energy applications. In this perspective, we have presented theoretical investigations focusing on the different types of double perovskite oxides based on the composition space in a systematic manner. Corresponding electronic and optical properties are discussed along with a future outlook on the novel routes to find efficient members in this family.

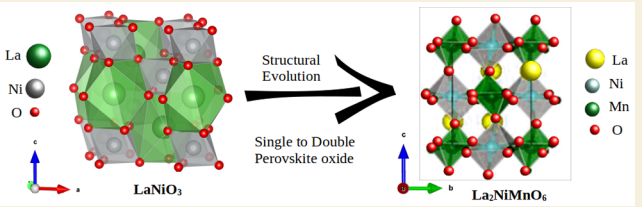

KEYWORDS: *double perovskite oxides, cation occupancy, alkaline-earth, transition metal, rare earth, mixed cation/anion*

INTRODUCTION

An increase in energy demand globally has inspired the research community to determine better materials for sustainable and clean energy along with reducing concerns about environmental pollution from fossil energy. In this regard, perovskite materials have been established as a family of materials for energy conversion and storage.[1−4] Any mineral with an ABX_3 structural framework is known as perovskite, with $CaTiO_3$ being the first to be discovered. Here, A is a cation, B is usually a metallic cation, and X is oxygen or halogen. Extensive studies on improving these perovskite materials have extrapolated into developing double perovskites with $A_2BB'X_6$ stoichiometry.[5] The oxide family of double persovskites with $A_2BB'O_6$ stoichiometry[6−8] have much advanced dominance in the field of energy harvesting, which includes solar cells, light-emitting diodes, and photocatalysis.[9,10] In the field of solar cells, the charge-carrier recombination can be envisaged, whereas in photocatalysis, the photoexcited electrons are the prominent governing factors. In this regard, double perovskite oxides (DPOs) have emerged as a promising materials family for such energy applications, while a profound understanding is required from the electronic structure perspective in order to explore their ability to be used as highly efficient photovoltaic and photocatalytic materials. We have witnessed a series of experimental and theoretical investigations on DPOs where the structural, electronic, and optical properties have been manifested in the last couple of decades. In this perspective, we have taken a constructive theoretical viewpoint regarding the electronic and optical properties of DPOs, while exploring the compositional space and stoichiometry of these materials classified as alkaline earth−transition metal−rare earth−mixed anion/cation-based DPOs. A schematic representation of the classification of DPOs in our perspective is shown in Figure 1.

In alkaline earth double perovskite oxides ($AA'BB'O_6$), the A- and A′-sites with a valence of +1/+2 belong to the first or second group of the periodic table (K, Ba, Sr, etc.), whereas B- and B′-sites mostly have variable oxidation states (+3, +4, +5, +6) combined stoichiometrically.[11,12] Apart from this, there is a constant ongoing effort to explore more of its electronic and optical properties through substitution of lighter elements, such as Sb, in place of heavier Bi. For exploring transition-metal-based DPOs, rare-earth-based DPOs, and mixed anion/cation DPOs, researchers have used a combinatorial approach having different proportions. Nowadays, due to data-driven research and development in the field of machine learning (ML) and artificial intelligence (AI), it is very much helpful to

Received: April 1, 2022
Revised: August 11, 2022
Accepted: August 12, 2022
Published: September 9, 2022

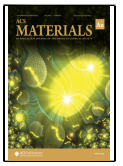

https://doi.org/10.1021/acsmaterialsau.2c00031
ACS Mater. Au 2022, 2, 655−664

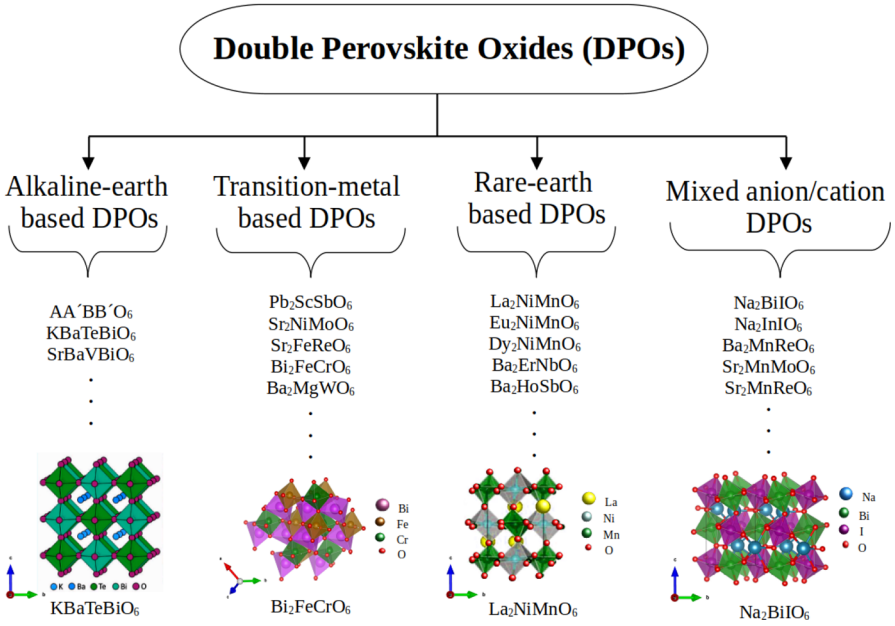

Figure 1. Representation of the classification of double perovskite oxides with the material class and pictorial representation of an example structure in each case.

study the feasibility and predict the properties of material computationally without it being synthesized physically, giving rise to a huge amount of research opportunity in these areas.

Advanced studies in perovskites reveals the new family of complex DPOs.[6,7] In general, the 3d and 4d electron configuration and their multivalency features make transition metal elements the best candidates to be occupied in the B-site cation position.[13−15] It is also worthy to note that the transition metal oxides exhibit perovskite-like structure and possess extensive physical properties, making the perovskite constituted with these transition elements a better solar-cell material.[16−19] Along with other components, the BX_6 octahedral tilt further stabilizes the perovskite oxide structure by lowering the crystal symmetry.[10] In addition, the cation ordering in such perovskites also plays a pivotal role in obtaining better stability.

Recently, tremendous efforts have been made to address the energy issues through developing new functional materials. Nevertheless, oxide perovskites and their derivatives have been extensively used in many technologies, reflecting their versatile properties.[9,10] Due to their compositional and structural flexibility, oxide perovskites show several other attractive properties including superconductivity, ferroelectricity, magnetoresistance, and ionic conductivity. Although halide perovskites[20] have shown considerable promise in photovoltaic (PV) applications due to their superior photovoltaic properties such as extremely high optical absorption coefficient, super long carrier diffusion length, and low-temperature solution processability, the practical use of it and its commercialization is still not always possible because of the instabilities associated with moisture, temperature, and other environmental factors. On the other hand, double perovskite oxides and their derivatives have shown greater applications in electrocatalysis, photocatalysis, and photovoltaics attributed to their superior stability. Here, we provide an overall perspective on the structural and compositional flexibility of DPOs and their derivatives. Further, we discuss the status of their applications in catalysis and photovoltaics. Finally, we also deliver a brief insight into potential DPO-based research fields one could consider exploring in the near future.

RECENT PROGRESS IN DOUBLE PEROVSKITE OXIDES

Alkaline-Earth-Based Double Perovskite Oxides

There are several types of complex oxide perovskites. One being the pyrochlore mineral family having the general formula $(Na,Ca)_2Nb_2O_6(OH)$. These pyrochlores can be subclassified as complex oxide perovskites with $A_2B_2O_6O'$ as the evolved formula.[21] Unlike usual perovskites, pyrochlores have two types of anions: one that links the A- and B-site (O) and the other that brings the link between the pair of A-sites (O′). The complex pyrochlore structure perovskites can be subcategorized in six ways: (1) $A_2B_2O_6$, obtained by a defective or vacant O′ oxide state; (2) $A_{2-x}B_2O_7$, arisen due to the partial occupancy of the A-site; (3) the neutral structure, caused by the O′-site occupying balancing anions along with the oxide ions; (4) $A_2B_2O_7$, due to the O′ migrating under constraints giving rise to partial occupancy for a previously unoccupied oxide site; (5) mixing of the A- and B-site metals; (6) AB_2O_6 β-pyrochlore, obtained with the metal in A-site residing on the O′-site.[11]

Another new family of complex double oxide perovskites, $AA'BB'O_6$ (A and A′ are univalent A-site cations; B and B′ are univalent B-site cations), have emerged from recent studies on lead-free perovskites.[12] This family of perovskites have proven its successful applications in photovoltaic and optoelectronic industries with improved stability and efficiency. In fact, compared to $A_2BB'O_6$, these $AA'BB'O_6$ materials are believed to possess lower band gap addition for improved photovoltaic applications. The same work[12] reports that with a simple charge balancing variation, 29,515 unique structures of $AA'BBiO_6$ DPOs can be obtained. Few of the structures can be obtained from the Inorganic Crystal Structure Database (ICSD). One such structure with high thermodynamic stability, $KBaTeBiO_6$, is the first one ever to be reported. In

https://doi.org/10.1021/acsmaterialsau.2c00031
ACS Mater. Au 2022, 2, 655−664

the work by Thind et al.,[12] among all the predicted compounds, only two compounds, $KBaTeBiO_6$ and $SrBaVBiO_6$, having negative formation enthalpy in their ground state and showing ideal perovskite structure, are lead-free. $SrBaVBiO_6$ has a flat valence band (VB) and conduction band (CB), making it a nonsuitable photovoltaic material. $KBaTeBiO_6$ has negative formation enthalpy of $\Delta H_f = -39$ meV/atom, suggesting it as an interesting system along with the feasibility of it to be synthesized. The same work also reports on the synthesis and analysis of $KBaTeBiO_6$ with a $P4/nmm$ space group and $a^0a^0c^0$ as the octahedral tilt pattern. The theoretical indirect band gap of $KBaTeBiO_6$ is reported to be 1.94 eV, whereas the experimental indirect band gap is found to be 1.88 eV. However, a theoretical direct band gap is found to be 2.83 eV occurring at Gamma-point. The work[12] also predicts that the band structure possesses highly dispersed valence and conduction bands, which are most desirable for faster transport of holes and electrons, making it more interesting. The effective mass of holes and electrons in $KBaTeBiO_6$ is calculated to be 0.25 and $0.28m_e$, respectively (where m_e is the mass of electrons). This low effective masses of holes and electrons contributes toward achieving better carrier transport. Furthermore, analysis of electronic properties in the $KBaTeBiO_6$ complex DPO has been discussed in the same work by Thind et al.[12] Presently, our group is working on further analysis of the system theoretically, and our computationally obtained results for total and projected density of states for $KBaTeBiO_6$ is shown in Figure 2. Analysis of the

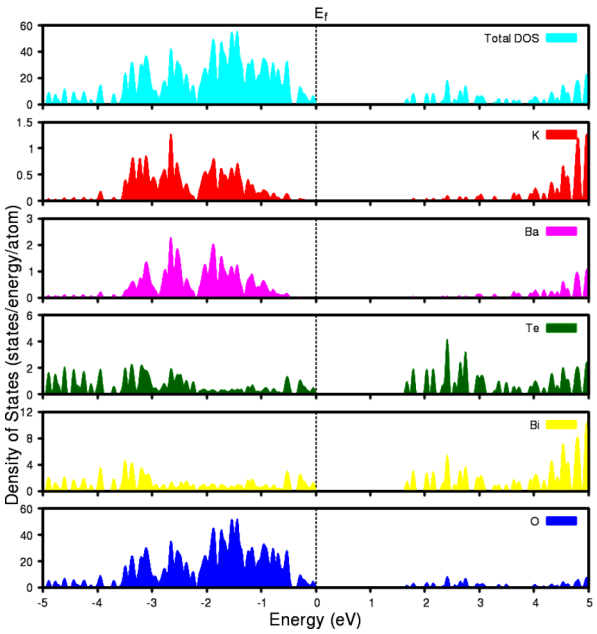

Figure 2. Computational analysis of $KBaTeBiO_6$ showing total and projected density of states.

partial density of states suggests that the O−2p and Bi−6s states contribute to the valence band regime with minor contribution from the Te−4d state, whereas the conduction band is dominated by Bi−6p and Te−5s states with the smaller occupancy by the O−2p state. The presence of the Bi−6s antibonding state in the valence band maxima rather than conduction band minima results in its +3 oxidation state. This oxidation state is further supported by 2.73*e* empty conduction band states of Bi. These aspects of Bi impact the defect tolerance due to the lone-pair chemistry.

Another interesting addition to the work[12] is the evaluation of another material configuration, $K_{0.625}Ba_{1.375}Te_{0.875}Bi_{1.125}O_6$. It is fascinating to see that without introducing any defect, this new nonstochiometric system exhibits a reduced band gap of 1.18 eV. The new system possesses the $P\bar{1}$ ground-state space group along with an $a^-b^-c^-$ octahedral tilt pattern. The new system also favors thermodynamic cation nonstoichiometry due to the calculated formation enthalpy of $\Delta H_f = -148$ meV/atom, lower than that of the pristine sample.[12] The efficiency of $KBaTeBiO_6$ is calculated to be 0.057%, which is relatively low; however, it shows much better stability than many other bismuth-based halide perovskites. Also, solar cells composed of $KBaTeBiO_6$ nanoparticles exhibit a performance similar to those based on high-quality thin films of other inorganic oxide perovskites. Much higher efficiency of the solar cells based on $KBaTeBiO_6$ can be achieved by controlling and optimizing the stoichiometry and growing high-quality thin films using aerosol-based technology.

Furthermore, studies have been carried out that effectively introduce pressure upon DPO materials in view of observing an enhanced properties regime such as inaccessible structural phase via temperature variation, Jahn−Teller distortions, band gap and photoluminescence evolution, as well as piezochromism.[22] In recent advances, pressure-induced evaluation of various properties in DPOs is an exciting field in terms of its structural evolution and usage in various energy applications.

Transition-Metal-Based Double Perovskite Oxides

Transition-metal-based double perovskite oxides are those in which the B-site cation is a transition metal such as Ni and Fe. Along with a number of exotic phenomena such as room temperature magnetoresistance, magneto-capacitance, and magnetostriction, these transition-metal-based DPOs exhibit other thought-provoking properties such as metallic/half-metallic ferromagnetism and magnetoresistance, as observed in Sr_2FeMoO_6, which is a half-metallic ferromagnet,[13] Sr_2FeReO_6, a half-metallic ferrimagnet,[14] and Sr_2FeWO_6, an antiferromagnetic insulator.[15]

Theoretical studies on lead-based DPOs, Pb_2ScSbO_6, have been reported by Hnamte et al.[24] Pb_2ScSbO_6 exhibits a face-centered cubic symmetry with a $Fm\bar{3}m$ space group. The material shows a direct band gap at 2.712 eV. This study also establishes the occurrence of a large number of density states at both VB and CB edges along with identifying the material as a semiconductor based on the band structure and optical absorption study.

The tetragonal Sr_2NiMoO_6 (SNMO) has been studied by Xu et al.[16] The structure studied shows an $I4/m$ space group. Sr ions are located between two types of corner-sharing octahedra, NiO_6 and MoO_6. SNMO nanoparticles crystallize in work-like nanograins with 20−50 nm diameters. The SNMO DPO structure exhibits indirect transitions with a band gap of 2.1 eV. The band structure analysis reveals that the VB is dominated by Ni−3d and O−2p from the MoO_6 octahedra, whereas the CB is dominated by Mo−5d and Ni−3d orbitals. Due to the position of the CB being more negative than the H_2O reduction energy, SNMO may split H_2O into H_2 with irradiation of visible light. In addition, O_2 evolution may also be observed since the VB is more positive than the O_2 oxidation energy. The photoluminescence study on SNMO shows an average lifetime of the system to be 11.2 μs.[16] This

https://doi.org/10.1021/acsmaterialsau.2c00031
ACS Mater. Au 2022, 2, 655−664

large carrier lifetime dictates the importance of Ni ions in delaying the recombination of excitons. A large carrier lifetime also serves as a benefit for the system to be used in photocatalysis. The photocatalytic activity in SNMO can be described from multivalent Ni^{2+}/Ni^{3+} and Mo^{6+}/Mo^{5+}, which may contribute to improving the photodegradation. A schematic of multivalent Mo and Ni ions in Sr_2NiMoO_6 is shown in Figure 3. Ni^{3+} and Mo^{5+} ions in SNMO act as a

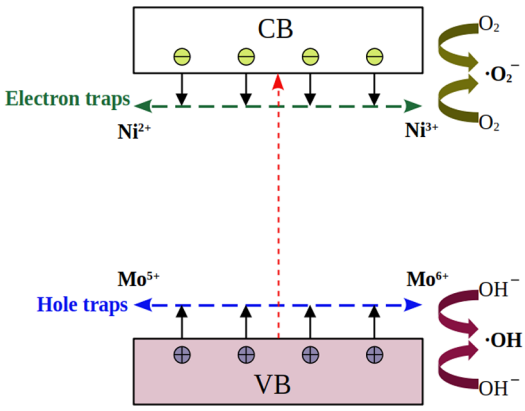

Figure 3. Schematic representation of multivalent Mo and Ni ions in transition-metal-based double perovskite oxide, Sr_2NiMoO_6.

donor and acceptor, respectively, altering the recombination of photocreated hole−electron pairs:

$$Mo^{6+} + e^{-}_{CB} \rightarrow Mo^{5+} \text{ electron trap}$$

$$Ni^{2+} + h^{+}_{VB} \rightarrow Ni^{3+} \text{ hole trap}$$

Rai et al. studied the magnetic properties of A_2FeReO_6 (A = Sr, Ba).[17] With the analysis of density of states (DOS) and band structure in A_2FeReO_6 (A = Sr, Ba), they clearly observed the ground state of Sr-based Sr_2FeReO_6 to be a ferrimagnetic metal with the Fe d states contributing a VBM at 2.0 eV and a CBM at 2.2 eV. However, the Fe−d states in Ba-based Ba_2FeReO_6 possess a bandwidth of about 4.6 eV spread between −2.30 and 2.4 eV. Both systems show an insulating nature in the spin-up state with a finite band gap corresponding to the split between occupied Fe/Re 3d−t_{2g} (d_{xy}, d_{yz}, d_{xz}) and unoccupied Fe/Re 3d−e_g ($d_{x^2-y^2}$, d_{z^2}) with the majority contribution from Re−d and Fe−d orbitals in CB and VB, respectively. However, in the spin-down state, the band structure shows broader bands, indicating its metallic behavior. Along with the broad bands, it also shows the Fermi energy, E_F, passing through the increasing peak, further establishing a confirmed spin-polarization at E_F, which is a signature of half-metallic materials. Interband transitions along the $\Delta-H$ symmetry takes place in these indirect band gap materials. The metallic behavior of this material is further validated by optical absorption analysis in which reflection is more prominently observed.

Song et al. discussed the Bi_2FeCrO_6 structure and its magnetic properties.[18] Various studies on Bi_2FeCrO_6[18,25,26] have shown that its ground-state structure exhibits a non-metallic $R3$ space group. The alternating rotations of O ions around Fe/Cr cations in FeO_6/CrO_6 octahedra, crystal field splitting, and spin exchange splitting lead the structure to displace from its cubic phase. The material has a semiconductor behavior with a band gap slightly larger than 0.26 eV formed between fully occupied Cr 3d−t_{2g} and unoccupied Fe 3d−t_{2g} bands. The magnetic order turns is ferrimagnetic with every Cr spin orienting upward and every Fe spin orienting downward. The Fe/Cr show high spin states along with a magnetic moment of $3.70\mu_B$ for the Fe sphere and $-2.18\mu_B$ in case of the Cr sphere, indicating its antiparallel nature, along with each Fe^{3+} and Cr^{3+} cation contributing 5 and $-3\mu_B$, respectively. The spin exchange interaction study of Bi_2FeCrO_6 among ferrimagnetic, ferromagnetic, and two magnetic orders obtained by reversing one of the two Cr/Fe spins in ferrimagnetic order was carried out by Song et al. The three magnetic structures, Fe−Cr, Fe−Fe, and Cr−Cr, have a ground-state energy of 310, 161, and 166 meV, respectively. The same work also supports the analysis of Curie temperature (T_C) based on Monte Carlo simulations and has a reported T_c value slightly higher than 450 K, which is consistent with other experimentally reported high Curie temperature values above room temperature.[27−31] However, few other works[25,26] reported obtaining a low Curie temperature of ≈130 K.

Dutta et al. reveals the study on $Ba_2(InM)O_6$ (M = Nb, Ta),[19] whereas Ting et al. reported $Ba_2(InNb)O_6$ (BIN) with a $Fm\bar{3}m$ crystal structure space group along with the lattice parameter of a = 8.2819 Å.[32,33] A work by Lufaso et al.[34] emphasizes the $Ba_2(InTa)O_6$ (BIT) system with a $Fm\bar{3}m$ space group and a lattice parameter of a = 8.2814 Å. However, Zurmühlen et al. report infrared reflectivity on both BIN and BIT.[35,36] The electronic property study on these materials shows that their electrical properties are highly influenced by the interaction between transition metal d orbitals and oxygen 2p orbitals. Yin et al.[37] have done an extensive study on BIN with both Raman scattering and UV−visible reflectance spectroscopy. In the work by Yin et al.,[37] different ionic radii of cations leading to distortion in the octahedron was reported. Three vibrational branches in the Raman spectra analogous to a stretching mode, bending mode, and external mode further aid the justification of octahedral distortion. The same work also establishes a report with the band gap of BIN at 3.82 eV based on UV−visible spectra. Work by Dutta et al. reveals the band structure of both BIN and BIT to be similar. Both of these structures exhibit a direct band gap at a high-symmetry Γ point. The band gaps of BIN and BIT are reported to be 2.75 and 3.5 eV, respectively. A comparative smaller band gap of BIN with BIT indicated the more covalent nature of Nb−O bond compared to the Ta−O bond. The static dielectric function (ε_0) is reported to be 4.8 and 4.3 for BIN and BIT, respectively.[19] We can also establish validation of the Penn model[38] by comparing the values of ε_0 being inversely proportional to the band gap, E_g. Based on optical function analysis, the static refractive index (n_0) is reported to be 2.2 and 2.1 for BIN and BIT, respectively.

There are several reported studies on Ba_2MgWO_6, among which Brik has reported a first-principles study,[23] whereas the first experimental studies have been reported in another work[39,40] which establishes the cubic phase of the material. The lattice constant of Ba_2MgWO_6 was found to be 8.016 Å.[23,41] The system exhibited an indirect band gap of 2.89 eV based on a theoretical study,[23] whereas it was reported to be 3.4 eV based on experimental observation.[42] The band structure of Ba_2MgWO_6 obtained theoretically is shown in Figure 4. The bottom of the CB mainly consists of W−5d orbitals, and the top of VB is dominated by O−2p orbitals.[23] The band structure analysis also reveals the presence of two sub-bands at the CB edge with a narrow gap of ≈1 eV. A lower

https://doi.org/10.1021/acsmaterialsau.2c00031
ACS Mater. Au 2022, 2, 655−664

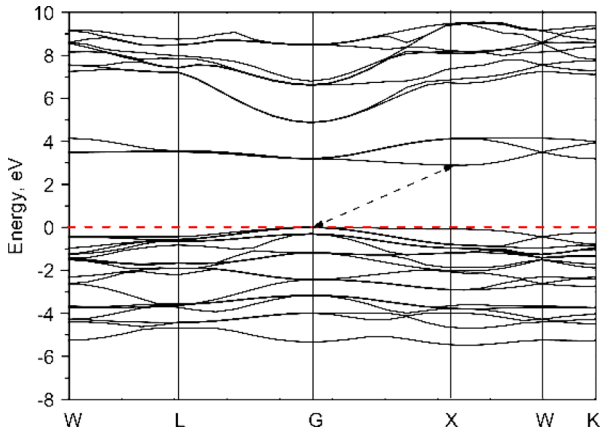

Figure 4. Band structure of transition-metal-based double perovskite oxide, Ba_2MgWO_6 showing indirect band gap. Adapted with permission from ref 23. Copyright 2012 Elsevier.

band observed in the range of 3.5−4.5 eV is closely flat in nature, indicating an inferior electron mobility, whereas the upper band lying between 5.5 and 9.5 eV reveals a more dispersed nature. The bonding of Mg and Ba ions with the Ba_2MgWO_6 crystal lattice is expected to be ionic in nature,[23] whereas that of composite WO_6 is found to be mostly covalent due to the considerable difference between the calculated and formal charges of the W/O ions. The same work[23] also reports the calculated refractive index (n_0) as 2 for Ba_2MgWO_6. The density of states analysis establishes transition from O−2p to W−5d orbitals at ∼5 eV, whereas transition from the O−2p to Ba−5d orbital occurs at 9 eV. Distinct work on pressure effects in Ba_2MgWO_6 has been studied by Brik,[23] which reveals the behavior of Ba_2MgWO_6 from a pressure of 0 to 30 GPa. The indication of pressure coefficient being 1 order of magnitude greater for the lattice constant than the W−O interatomic distance (0.0123 Å GPa^{-1} v/s 0.001 51 Å GPa^{-1}) acknowledges the rigidity in W−O compressibility. As the pressure increases, there is an observed decrease in lattice constant, which is credited to the WO_6 octahedra shifting closer to each other. The major ionic nature in the case of Ba−O and Mg−O causes these bonds to exhibit easy compressibility compared to that with the covalently interacting W−O bonds. Pressure coefficients for Ba−O and Mg−O distances are similar to the values of 0.00438 and 0.00464 Å GPa^{-1}, respectively. Another important pressure manifestation in Ba_2MgWO_6 is the linear evolution of the band gap with a pressure coefficient of 0.006 01 eV GPa^{-1}.

Previous works on Sr_2FeMO_6 (M = Mo, W, Re)[13−15] reveal the crystal structures of all three systems to be cubic in nature with Fe−M distances of 3.945, 3.975, and 3.945 Å, respectively. The same works also establish the FeM valence to be +8; that is, the number of d electrons per FeMo and FeW is found to be 6, whereas it is 7 in case of FeRe. In both ferromagnetic and antiferromagnetic states, five electrons fill and complete the majority of spin bands of Fe, while the minority of spin bands in both M = Mo, W contain one electron and M = Re holds two electrons. Further, the Curie temperatures of SFMO and SFRO materials are found to be 419 and 401 K, respectively.[13,15] The cause for this large magnetic transition temperature was predicted by Sarma et al.,[43] as the huge interatomic exchange coupling strength, J, between Fe and M and the low intra-atomic exchange (between M and M) strength I gives the robust intensified effective exchange at Mo due to the Fe 3d and Mo 4d hybridization. Both SFMO and SFRO may be considered as ferrimagnetic materials in nature since the magnetic moments of Fe in both the materials are aligned ferromagnetically, whereas Mo and Re exhibit induced magnetic moments which are coupled antiferromagnetically to Fe moments. However, these materials are categorized as ferromagnetic due to the fact that Mo and Re are nonmagnetic by their very nature and their antiparallel moments are induced by Fe moments via 4d/5d−3d hybridization. An interesting, yet contradicting, phenomenon of the antiferromagnetic nature with very low Néel temperature of 16−37 K occurs in a similar structure, Sr_2FeWO_6(SFWO), despite W being a 5d equivalent of Mo and occupying a position next to Re in the periodic table. Extrapolating Sarma's prediction in the work,[43] Kanamori et al. gave a generalized mechanism, now termed as Kanamori and Terakura mechanism,[44] followed by Fang et al. who established a new mechanism on strong ferromagnetic stabilization in these materials.[45] In this work, they successfully showed that stronger hybridization of O−2p with W−5d in the case of SFWO compared to that with the O−2p−Mo−4d hybridization in SFMO is the main source in lifting W 5d orbitals to higher energy, in turn paralyzing the ferromagnetic equalization. However, in the case of SFRO, the deeper Re−5d orbitals compared to W cancel the intensified p−d hybridization and rebuilds the ferromagnetic stabilization within the system.

Owing to its intensified magnetic properties, these transition-metal-based DPOs are suitable for spintronics. One could certainly look upon these type of materials for magnetization-related studies. It is a fascinating field to study the structural evolution of materials by application of external stimuli and its consequence on magnetic properties. The possibility of catalysis in these materials is also another view one could look upon.

Rare-Earth-Based Double Perovskite Oxides

Rare-earth (RE, also called as lanthanide)-based DPOs are of the form $A_2B'B''O_6$. This wider group is further classified into two subgroups based on the RE elemental occupancy site. One group falls under the RE element occupying the A-site in which the B′ and B″-site will be employed by transition-metal cations such as Ni or Mn. Another subgroup takes up the RE element at the B′- and/or B′′-site(s), whereas alkaline-earth metal such as Ba fits into the A-site. Recently, these DPOs have gained prominent interest among materialists due to their unique control over magnetic behavior, optical properties, and charge transfer.

RE Element Occupying the A-Site. The study by Sheikh et al.[47] reports on RE-based DPO, RE_2NiMnO_6 (RE = La, Eu, Dy, Lu) (RENMO). Out of the four, three structures, ENMO, DMNO, and LuNMO show crystallization in the $P2_1/m$ monoclinic phase, whereas LaNMO exhibits 44.36% crystallization in the $P2_1/n$ monoclinic space group and 55.64% crystallization in the $R\bar{3}$ rhombohedral space group. The Mn−O−Ni bond angle gradually decreases from 166.37° in LaNMO to 145.50° in LuNMO, accounting for an increased octahedral distortion and decreased tolerance factor. However, the average grain size of these structures increases from LaNMO to LuNMO in the order of 190 to 560 nm, respectively. The optical band gap of all four structures, RENMO (RE = La, Eu, Dy, Lu), are in a range similar to that of silicon (≈1.1 eV), showing their characteristics of being

https://doi.org/10.1021/acsmaterialsau.2c00031
ACS Mater. Au 2022, 2, 655−664

usable in photovoltaic applications. The observed band gap of LaNMO, ENMO, DNMO, and LuNMO is 1.08, 1.1, 1.19, and 1.12 eV, respectively. The analysis on charge carrier lifetime based on the frequency-dependent Bode plot in RENMO (RE = La, Eu, Dy, Lu) is reported to be 0.022, 0.110, 0.108, and 0.076 ms, respectively, establishing RENMO as useful for the photovoltaics industry. The same work[47] also analyses the $J-V$ characteristics of RENMO (RE = La, Eu, Dy, Lu). The combined effect of low series resistance (R_S) and charge-transfer resistance (R_{CT}) along with a high recombination resistance (R_{rec}) in LaNMO makes it the best candidate for solar cells among all four fabricated RENMO structures, with a 0.17% power conversion efficiency.

An interesting ferromagnetic material series, RE_2NiMnO_6 (RE = La, Pr, Sm, Tb) (RENMO), have been studied by Lekshmi et al.[46] The polycrystalline RE_2NiMnO_6 (RE = La, Pr, Sm, Tb) has a $P2_1/n$ monoclinic space group. In addition, there exists an observed decrease in lattice parameter, unit cell volume and bond angles in RENMO with a decrease in RE ionic radii. The unit cell parameter including cell volume and bond angle with respect to RE ionic radii is shown in Figure 5a.

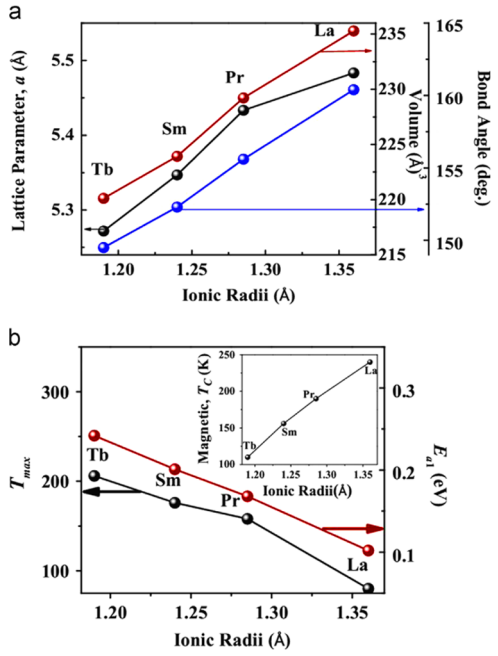

Figure 5. (a) Representation of the change in unit cell parameter including cell volume and bond angle with RE ionic radii. (b) Variation of T_{max} of $\tan\delta(T)$ and $E_{\alpha 1}$ with RE ionic radii. Inset: Evolution of magnetic T_C with RE ionic radii. Adapted with permission from ref 46. Copyright 2014 Elsevier.

The study involving thermo-magnetization for the RE_2NiMnO_6 (RE = La, Pr, Sm, Tb) compound has been reported,[46] wherein the material magnetization was reported with a temperature range of 10−300 K. It is interesting to know that all four compounds show paramagnetic to ferromagnetic transitions at higher temperature (>100 K). Sm_2NMO and Tb_2NMO exhibit a magnetic transition at 160 and 110 K, respectively. This is followed by a re-entrant magnetic transition at a low temperature of 20 and 12 K, respectively. The presence of inherent coupling of the Ni−Mn network along with the RE^{3+} ion[48,49] might be the probable cause of the low-temperature re-entrant nature.[50] A decrease in ionic radii from LaNMO to TbNMO also contributes to the systematic decrease in their Curie temperature (T_C). However, T_{max} and $E_{\alpha 1}$ show an indirect proportionality with ionic radii of RE, indicating that electron hopping between Ni and Mn is more suppressed with decreasing RE ionic radii. Variation of T_{max} with respect to ionic radii is shown in Figure 5b. The tendency of coupling between magnetic and dielectric properties of RENMO implies a spin−lattice coupling, opening more research areas in spintronics. However, the double transition at ≈160 and ≈240 K reported for disordered La_2NiMnO_6 makes it an interesting compound. Even though highly ordered La_2NiMnO_6 exhibits a magnetic transition only at a high temperature of 270 K,[51] its disordered phase also exhibits a magnetic transition at a relatively lower temperature of ≈150 K due to the strong superexchange interaction between $Ni^{3+}-O-Mn^{3+}$ bonds. This unclear nature of two magnetic transitions in La_2NiMnO_6 further opens up several research opportunities in this direction.

RE Element Occupying the B-Site. The electrical transport mechanism in Ba_2ErNbO_6 (BEN) was reported by Mukherjee et al.[52] The cubic perovskite BEN crystallizes in the $Fm\bar{3}m$ space group along with a tolerance factor value of T_f = 0.98, furthermore establishing its cubic structure. The average grain size of BEN is ≈1.5 μm via scanning electron microscopy. ErO_6 and NbO_6 octahedra in BEN do not show tilting in any direction, which can be represented as $a^0a^0a^0$ in Glazer notation.[53−55] Two well-defined bands found in the infrared (IR) spectrum vibrational mode at 387 and 600 cm^{-1} represent asymmetric bending and asymmetric stretching of NbO_6 octahedron, respectively, whereas a weak band at 846 cm^{-1} is due to the symmetric stretching in the NbO_6 octahedra. In addition, a dip in the IR region's vibrational mode at 418 cm^{-1} is observed, corresponding to the stretching of ErO_6 octahedra. Further, the work also reports the activation energy of BEN as E_a = 0.85 eV along with the relaxation time corresponding to the frequency-dependent dielectric loss obeying the Arrhenius law.

The structural study on Ba_2RESbO_6 (RE = Er, Ho) was carried out by Halder et al.[56] Both Ba_2ErSbO_6 (BES) and Ba_2HoSbO_6 (BHS) systems were found to have cubic symmetry with a $Fm\bar{3}m$ space group. Lattice parameters of BES and BHS were 8.4036 and 8.3908 Å, respectively. Density of states analysis[56] shows that electronic properties of both BES and BHS are governed by the interaction between transition metal d orbitals, rare-earth ion f orbitals, and oxygen 2p orbitals. Interestingly, both BES and BHS exhibit similar band profiles. BES and BHS possess a direct band gap along the highly symmetric Γ−Γ points with a band gap value of 2.2 and 3.45 eV, respectively. The desired nature of direct Γ−Γ transitions gives these materials potential in the optoelectronics industry for fabricating laser diodes and light-emitting diodes in visible and ultraviolet regions. The static refractive index n_0 for BES and BHS was found to be 1.87 and 2.11, respectively, whereas the calculated static dielectric constant $\varepsilon(0)$ was found to be 3.48 and 4.52, respectively. Based on the Born effective charge (BEC) analysis,[56] we can clearly see larger BEC values for rare earth elements (Er, Ho) and Sb ions, indicating its behavior as a donor, whereas the smaller BEC value in case of O ions indicates its behavior as an acceptor, due to which the charge transfer occurs from Ho, Er, or Sb to O ions.

Rare-earth-based DPOs have applications in various fields such as optoelectronic and photovoltaic industries. A huge

https://doi.org/10.1021/acsmaterialsau.2c00031
ACS Mater. Au 2022, 2, 655−664

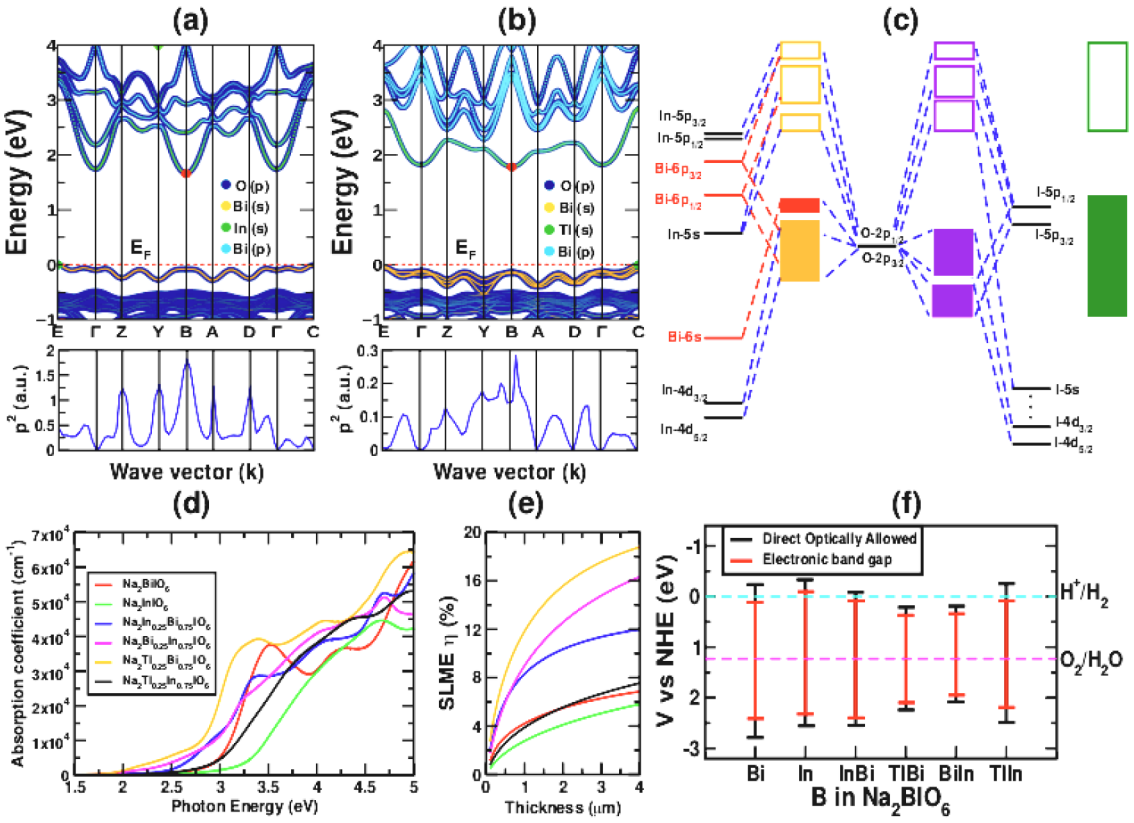

Figure 6. Band structure and optical transition probability (p^2) between an allowed band at the minimum band gap in (a) $Na_2Bi_{0.25}In_{0.75}IO_6$ and (b) $Na_2Tl_{0.25}Bi_{0.75}IO_6$. (c) Representation of molecular orbitals for $Na_2Bi_{0.25}In_{0.75}IO_6$, where empty and filled boxes specify unoccupied conduction bands and occupied valence bands. (d) Computed absorption coefficient spectra. (e) Spectroscopic limited maximum efficiency versus thickness of the material at 298 K for pristine and mixed compounds. (f) Band-edge positions with respect to water redox levels for Na_2BIO_6 (B = Bi, In, $In_{0.25}Bi_{0.75}$) marked on the *x*-axis as $Tl_{0.25}Bi_{0.75}$ (TlBi), $Bi_{0.25}In_{0.75}$ (BiIn), $Tl_{0.25}In_{0.75}$ (TlIn). Adapted from ref 57. Copyright 2020 American Chemical Society..

scope is oriented toward the study of magnetic transitions in these materials, which could be established in the field of spintronics. Many unknown attributes underlying magnetic phenomena disclose several new opportunities for materialists to look into.

Mixed Cationic/Anionic Double Perovskite Oxides

Apart from pure DPOs, mixed cationic/anionic DPOs have emerged as powerful materials that exhibit interesting properties which are highly influential in achieving usable materials as photoanodes in photochemical and photoelectrochemical water splitting as well as in spintronics.

Analysis by Kangsabanik et al.[57] not only reveals the understanding of new Na_2BIO_6 (B = Bi, In) DPOs but also constructs the orbital engineering approach for band gap tuning. Interesting structural observation in $ANaIO_6$ (A = Sr, Ca, Pb), where octahedral distortion is due to the Na atomic radii that lies exactly between that of Sr and Ca, both of which possess a monoclinic $P2_1/n$ space group that can also be seen in same work. From the structural analysis, among all of the structures, only Na_2BIO_6 (B = Bi, In) is reported to be stable in the monoclinic $P2_1/n$ phase. The highly covalent nature of Bi−O bonding in Na_2BiIO_6 (NBIO) compared to that of In−O in Na_2InIO_6 (NIIO) leads to higher orbital overlap in the case of NBIO, giving rise to more dispersive valence bands. NBIO possess an indirect band gap of 2.33 eV at highly symmetric C and A points for VBM and CBM, respectively, whereas NIIO has a direct band gap of 2.48 eV at the highly symmetric Γ point. In further analysis, Bi substitution in the case of NIIO ($Na_2Bi_{0.25}In_{0.75}IO_6$) observes the introduction of hybridization between lone pair Bi 6s and O 2p orbitals, which, in turn, establishes the reduction in band gap to 1.66 eV, as shown in Figure 6. This new Bi-substituted NIIO compound possesses both an ideal band gap as well as a dispersive band structure that is essential for photovoltaic applications. Although Tl is toxic, it is substituted for NBIO mainly to validate the orbital-engineering method. This new compound, $Na_2Tl_{0.25}Bi_{0.75}IO_6$, exhibits an intermediate band below the CBM consisting of Tl s states, helping to reduce the indirect band gap for 1.78 eV, shown in Figure 6. Better absorption characteristics and dispersed band-edges make these compounds applicable in the photovoltaics industry, whereas the position of the VBM, which is the occurrence of oxygen evolution reaction (OER), efficiently makes the materials useful as photoanodes in photochemical and photoelectrochemical (PEC) water splitting. Promising optical absorption, highly dispersive band-edges, and well positioned VBM for efficient OER make the substituted compounds potential candidates for PC/PEC applications.

A family of DPOs, $A_2BB'O_6$ (A = Ba, Sr) (BB′ = FeRe, MnMo, MnRe) were studied by Ali et al.[58] Interestingly, all of these DPOs exhibit a cubic structure with the $Fm\bar{3}m$ space group at ambient temperature. The bond lengths calculated between B−O and B′−O indicate that the $B'O_6$ octahedra are marginally smaller than the BO_6 octahedra. Analysis by Ali et al.[58] on $A_2BB'O_6$ (A = Ba, Sr) (BB′ = FeRe, MnMo, MnRe)

https://doi.org/10.1021/acsmaterialsau.2c00031
ACS Mater. Au 2022, 2, 655−664

reported both a generalized gradient approximation (GGA) approach as well as a GGA+U approach. The GGA-based approach showed d−d hybridization between FeRe, MnMo, and MnRe in both spin-up and spin-down states, indicating the metallic nature of all of these compounds; the GGA+U-based approach emphasized only Ba_2FeReO_6, Sr_2MnMoO_6, and Sr_2MnReO_6 to be metallic, whereas Ba_2MnReO_6, Ba_2MnMoO_6, and Sr_2FeReO_6 to be half-metallic. Spin−orbit coupling (SOC), including a GGA+U approach, discovers further interesting observations that indicate all the structures to be metallic in nature. Since SOC becomes a crucial factor to be considered during the presence of heavy elements such as Ba and Re, we may conclude that the results based on SOC included GGA+U; that is, all structures showing a metallic nature were more accurate. The Fermi region of all of the structures is mainly occupied by BB′ ions, which is mainly d state orbitals. The study on charge density by Ali et al.[58] reveals the covalent bonding between B/B′ with O atoms driven by the strong hybridization between cationic d orbitals and anionic p orbitals, whereas the ionic bond existing between Mn and O has been studying based on its electronegativity. The same study also shows that the ionic nature of O with alkaline earth metal decreases from Ba to Sr in $A_2BB'O_6$ (A = Ba, Sr) (BB′ = FeRe, MnMo, MnRe). In addition, all of the considered systems in $A_2BB'O_6$ (A = Ba, Sr) (BB′ = FeRe, MnMo, MnRe) exhibit ferromagnetic behavior with high magnetic moments.

The study of hybrid materials has always been exciting in glazing intermediate regimes, and these mixed cations/anions definitely serve as one such group. With the interplay of cation/anion composition space, much more advanced phenomena with respect to all electronic, optical, and magnetic properties are expected. Further studies on these materials are in the limelight for establishing much better materials with flexibility of structural deformation along with use in various applicational fields such as catalysis and water splitting and is certainly an open field to seek new materials.

FUTURE OUTLOOK AND SUMMARY

In this perspective, we have discussed how to exploit the double perovskite oxides and their derivatives for widespread applications and provided an outlook on the challenges and opportunities that lie ahead for this enticing class of compounds. We posit that this class of materials has enormous potential for the future development of multidisciplinary research combining spintronics, electronics, and photonics. This perspective attempts to describe how the properties of DPOs are tuned for specific applications. Compositional tuning and band gap engineering are extensively used techniques due to the flexibility of the perovskite structure. Though a lot of research has already been done on bulk perovskite, layered and heterostructure-combined perovskites have not been thoroughly looked at by the scientific community. Without distorting the advantages of oxide perovskite structures and properties, we have addressed how the shortcomings of corresponding applications are now a major challenge for the scientific community. An extensive approach involving passivation, intrinsic material stability, and doping strategies needs to be adopted to overcome the shortcomings of DPOs.

The synergistic effect in terms of electronic and optical properties of the individual double perovskite oxides could be amplified further when the corresponding heterostructure can be constructed from them. In this regard, theoretical insight would be influential to predict new combinations of DPOs for efficient heterostructure material. The theoretical investigation also facilitates resolving lattice mismatch in individual oxide perovskites for heterostructure construction. Another route for efficient and novel DPOs is through exerting hydrostatic pressure. This would certainly pave the way to find new compositions and stoichiometries that might be difficult to synthesize in laboratory. The electronic and optical properties can be tuned under the influence of external strain, and researchers can further try to expand the possibility of finding new stable and good-performing materials which could later be synthesized and put into practical use. One can also perform a systematic high-throughput screening based on electronic and optical properties to find a promising double perovskite oxide material for applications in photovoltaics and photocatalysis. Magnetic properties are known to be seen in oxide perovskites, and DPOs have already proven to have varied magnetic properties. Transition-metal-based DPOs are exceptionally well-suited materials for the study of magnetic behavior and for further applications in spintronics. DPOs span various categories both in terms of understanding fundamental phenomena as well as in application-oriented tasks and, thus, create immense research opportunities. Overall, there is a huge potential in the double perovskite oxide family that can be manifested further while tuning the underlying electronic and optical properties.

AUTHOR INFORMATION

Corresponding Author

Sudip Chakraborty − *Materials Theory for Energy Scavenging (MATES) Lab, Harish-Chandra Research Institute (HRI), A CI of Homi Bhabha National Institute, Prayagraj, India 211019*; orcid.org/0000-0002-6765-2084; Email: sudipchakraborty@hri.res.in, sudiphys@gmail.com

Author

Manasa G. Basavarajappa − *Materials Theory for Energy Scavenging (MATES) Lab, Harish-Chandra Research Institute (HRI), A CI of Homi Bhabha National Institute, Prayagraj, India 211019*

Complete contact information is available at: https://pubs.acs.org/10.1021/acsmaterialsau.2c00031

Author Contributions

CRediT: **Manasa G Basavarajappa** writing-original draft (equal), writing-review & editing (equal); **Sudip Chakraborty** conceptualization (lead), supervision (equal), writing-original draft (equal), writing-review & editing (equal).

Notes

The authors declare no competing financial interest.

ACKNOWLEDGMENTS

M.G.B. and S.C. are thankful to the institute PhD fellowship of HRI and HBNI. S.C. would like to acknowledge HRI Prayagraj and DST-SERB Funding (SRG/2020/001707) for the infrastructure and funding.

REFERENCES

(1) Goldschmidt, V. M. Die Gesetze der Krystallochemie. *Die Naturwissenschaften* **1926**, *14*, 477−485.

(2) Hoskin, P. W. O. In *Minerals: Their Constitution and Origin*; Wenk, H.-R., Bulakh, A. G., Eds.; Cambridge University Press: Cambridge, U.K., 2004.
(3) Szuromi, P.; Grocholski, B. Natural and engineered perovskites. *Science* **2017**, *358*, 732−733.
(4) Kumar, V.; Singh, S. Improved structure stability, optical and magnetic properties of Ca and Ti co-substituted BiFeO3 nanoparticles. *Appl. Surf. Sci.* **2016**, *386*, 78−83.
(5) Patterson, F. K.; Moeller, C. W.; Ward, R. Magnetic Oxides of Molybdenum(V) and Tungsten(V) with the Ordered Perovskite Structure. *Inorg. Chem.* **1963**, *2*, 196−198.
(6) Anderson, M.; Greenwood, K.; Taylor, G.; Poeppelmeier, K. B-cation arrangements in double perovskites. *Prog. Solid State Chem.* **1993**, *22*, 197−233.
(7) Zhao, F.; Yue, Z.; Gui, Z.; Li, L. Preparation, Characterization and Microwave Dielectric Properties of A2BWO6(A = Sr, Ba ; B = Co, Ni, Zn) Double Perovskite Ceramics. *Jpn. J. Appl. Phys.* **2005**, *44*, 8066−8070.
(8) Barnes, P. W.; Lufaso, M. W.; Woodward, P. M. Structure determination of A2M3+TaO6 and A2M3+NbO6 ordered perovskites: octahedral tilting and pseudosymmetry. *Acta Crystallographica Section B Structural Science* **2006**, *62*, 384−396.
(9) Vasala, S.; Karppinen, M. A2B'B"O6 perovskites: A review. *Prog. Solid State Chem.* **2015**, *43*, 1−36.
(10) Yin, W.-J.; Weng, B.; Ge, J.; Sun, Q.; Li, Z.; Yan, Y. Oxide perovskites, double perovskites and derivatives for electrocatalysis, photocatalysis, and photovoltaics. *Energy Environ. Sci.* **2019**, *12*, 442−462.
(11) Roth, R.; Vanderah, T.; Bordet, P.; Grey, I.; Mumme, W.; Cai, L.; Nino, J. Pyrochlore formation, phase relations, and properties in the CaO−TiO2−(Nb,Ta)2O5 systems. *J. Solid State Chem.* **2008**, *181*, 406−414.
(12) Thind, A. S.; Kavadiya, S.; Kouhnavard, M.; Wheelus, R.; Cho, S. B.; Lin, L.-Y.; Kacica, C.; Mulmudi, H. K.; Unocic, K. A.; Borisevich, A. Y.; Pilania, G.; Biswas, P.; Mishra, R. KBaTeBiO6: A Lead-Free, Inorganic Double-Perovskite Semiconductor for Photovoltaic Applications. *Chem. Mater.* **2019**, *31*, 4769−4778.
(13) Kobayashi, K.-I.; Kimura, T.; Sawada, H.; Terakura, K.; Tokura, Y. Room-temperature magnetoresistance in an oxide material with an ordered double-perovskite structure. *Nature* **1998**, *395*, 677−680.
(14) Kobayashi, K.-I.; Kimura, T.; Tomioka, Y.; Sawada, H.; Terakura, K.; Tokura, Y. Intergrain tunneling magnetoresistance in polycrystals of the ordered double perovskiteSr2FeReO6. *Phys. Rev. B* **1999**, *59*, 11159−11162.
(15) Kobayashi, K.-I.; Kimura, T.; Tomioka, Y.; Sawada, H.; Terakura, K.; Tokura, Y. Intergrain tunneling magnetoresistance in polycrystals of the ordered double perovskiteSr2FeReO6. *Phys. Rev. B* **1999**, *59*, 11159−11162.
(16) Xu, L.; Wan, Y.; Xie, H.; Huang, Y.; Yang, L.; Qin, L.; Seo, H. J. Synthesis, surface structure and optical properties of double perovskite Sr2NiMoO6 nanoparticles. *Appl. Surf. Sci.* **2016**, *389*, 849−857.
(17) Rai, D.; Shankar, A.; Ghimire, M.; Sandeep; Thapa, R. The electronic, magnetic and optical properties of double perovskite A2FeReO6 (A = Sr, Ba) from first principles approach. *Comput. Mater. Sci.* **2015**, *101*, 313−320.
(18) Song, Z.-W.; Liu, B.-G. Electronic structure and magnetic and optical properties of double perovskite Bi2FeCrO6from first-principles investigation. *Chinese Physics B* **2013**, *22*, 047506.
(19) Dutta, A.; Sinha, T. First principles study of electronic structure and optical properties of double perovskite Ba2(InM)O6 [, Ta]. *Solid State Commun.* **2010**, *150*, 1173−1177.
(20) Sarangi, A.; Basavarajappa, M. G.; Chakraborty, S. Tuning composition space in lead-free divalent and tetravalent halide perovskite: a critical review. *Emergent Materials* **2021**, 1−12.
(21) Modeshia, D. R.; Walton, R. I. Solvothermal synthesis of perovskites and pyrochlores: crystallisation of functional oxides under mild conditions. *Chem. Soc. Rev.* **2010**, *39*, 4303.
(22) Basavarajappa, M. G.; Nazeeruddin, M. K.; Chakraborty, S. Evolution of hybrid organic−inorganic perovskite materials under external pressure. *Applied Physics Reviews* **2021**, *8*, 041309.
(23) Brik, M. First-principles calculations of electronic, optical and elastic properties of Ba2MgWO6 double perovskite. *J. Phys. Chem. Solids* **2012**, *73*, 252−256.
(24) Hnamte, L.; Joshi, H.; Rai, D.; Thapa, R. Electronic and optical properties of double perovskite oxide Pb2ScMO6 (M = Ta, Sb) using a first principles approach. *J. Phys. Chem. Solids* **2019**, *129*, 188−195.
(25) Baettig, P.; Spaldin, N. A. Ab initio prediction of a multiferroic with large polarization and magnetization. *Appl. Phys. Lett.* **2005**, *86*, 012505.
(26) Baettig, P.; Ederer, C.; Spaldin, N. A. First principles study of the multiferroicsBiFeO3,Bi2FeCrO6, andBiCrO3: Structure, polarization, and magnetic ordering temperature. *Phys. Rev. B* **2005**, *72*, 214105.
(27) Nechache, R.; Harnagea, C.; Pignolet, A.; Normandin, F.; Veres, T.; Carignan, L.-P.; Ménard, D. Growth, structure, and properties of epitaxial thin films of first-principles predicted multiferroic Bi2FeCrO6. *Appl. Phys. Lett.* **2006**, *89*, 102902.
(28) Kamba, S.; Nuzhnyy, D.; Nechache, R.; Závěta, K.; Nižňanský, D.; Šantavá, E.; Harnagea, C.; Pignolet, A. Infrared and magnetic characterization of multiferroic Bi2FeCrO6 thin films over a broad temperature range. *Phys. Rev. B* **2008**, *77*, 104111.
(29) Nechache, R.; Harnagea, C.; Carignan, L.-P.; Gautreau, O.; Pintilie, L.; Singh, M. P.; Ménard, D.; Fournier, P.; Alexe, M.; Pignolet, A. Epitaxial thin films of the multiferroic double perovskite Bi2FeCrO6 grown on (100)-oriented SrTiO3 substrates: Growth, characterization, and optimization. *J. Appl. Phys.* **2009**, *105*, 061621.
(30) Aïssa, B.; Nechache, R.; Therriault, D.; Rosei, F.; Nedil, M. High-frequency electromagnetic properties of epitaxial Bi2FeCrO6 thin films grown by pulsed laser deposition. *Appl. Phys. Lett.* **2011**, *99*, 183505.
(31) Nechache, R.; Harnagea, C.; Pignolet, A. Multiferroic properties—structure relationships in epitaxial Bi2FeCrO6thin films: recent developments. *J. Phys.: Condens. Matter* **2012**, *24*, 096001.
(32) Ting, V.; Liu, Y.; Withers, R.; Krausz, E. An electron diffraction and bond valence sum study of the space group symmetries and structures of the photocatalytic 1:1 ordered A2InNbO6 double perovskites (A = Ca2+, Sr2+, Ba2+). *J. Solid State Chem.* **2004**, *177*, 979.
(33) Ting, V.; Liu, Y.; Withers, R.; Norén, L.; James, M.; Fitz Gerald, J. A structure and phase analysis investigation of the "1:1" ordered A2InNbO6 perovskites (A = Ca2+, Sr2+, Ba2+). *J. Solid State Chem.* **2006**, *179*, 551−562.
(34) Lufaso, M. W.; Barnes, P. W.; Woodward, P. M. Structure prediction of ordered and disordered multiple octahedral cation perovskites using SPuDS. *Acta Crystallographica Section B Structural Science* **2006**, *62*, 397−410.
(35) Zurmühlen, R.; Petzelt, J.; Kamba, S.; Voitsekhovskii, V. V.; Colla, E.; Setter, N. Dielectric spectroscopy of Ba(B1/2'B1/2')O3complex perovskite ceramics: Correlations between ionic parameters and microwave dielectric properties. I. Infrared reflectivity study (1012−1014 Hz). *J. Appl. Phys.* **1995**, *77*, 5341−5350.
(36) Zurmühlen, R.; Petzelt, J.; Kamba, S.; Kozlov, G.; Volkov, A.; Gorshunov, B.; Dube, D.; Tagantsev, A.; Setter, N. Dielectric spectroscopy of Ba(B1/2'B1/2')O3complex perovskite ceramics: Correlations between ionic parameters and microwave dielectric properties. II. Studies below the phonon eigenfrequencies (102−1012 Hz). *J. Appl. Phys.* **1995**, *77*, 5351−5364.
(37) Yin, J.; Zou, Z.; Ye, J. Photophysical and photocatalytic properties of the visible-light-driven photocatalysts BaIn0.5Nb0.5O3, BaCo1/3Nb2/3O3 and BaNi1/3Nb2/3O3. *Res. Chem. Intermed.* **2005**, *31*, 463−475.
(38) Penn, D. R. Wave-Number-Dependent Dielectric Function of Semiconductors. *Phys. Rev.* **1962**, *128*, 2093.
(39) Meenakshi, S.; Vijayakumar, V.; Achary, S.; Tyagi, A. High pressure investigation on double perovskite Ba2MgWO6. *J. Phys. Chem. Solids* **2011**, *72*, 609−612.

https://doi.org/10.1021/acsmaterialsau.2c00031
ACS Mater. Au 2022, 2, 655−664

(40) Steward, E. G.; Rooksby, H. P. Pseudo-cubic alkaline-earth tungstates and molybdates of theR3MX6type. *Acta Crystallogr.* **1951**, *4*, 503−507.
(41) Pychlau, P. Another method of calibration for low energy X-ray beams. *Phys. Med. Biol.* **1974**, *19*, 386−386.
(42) Eng, H. W.; Barnes, P. W.; Auer, B. M.; Woodward, P. M. Investigations of the electronic structure of d0 transition metal oxides belonging to the perovskite family. *J. Solid State Chem.* **2003**, *175*, 94−109.
(43) Sarma, D. D.; Mahadevan, P.; Saha-Dasgupta, T.; Ray, S.; Kumar, A. Electronic Structure ofSr2FeMoO6. *Phys. Rev. Lett.* **2000**, *85*, 2549−2552.
(44) Kanamori, J.; Terakura, K. A General Mechanism Underlying Ferromagnetism in Transition Metal Compounds. *J. Phys. Soc. Jpn.* **2001**, *70*, 1433−1434.
(45) Fang, Z.; Terakura, K.; Kanamori, J. Strong ferromagnetism and weak antiferromagnetism in double perovskites:Sr2FeMO6(M = Mo,W, and Re). *Phys. Rev. B* **2001**, *63*, 180407.
(46) Lekshmi, P. N.; Vasundhara, M.; Varma, M. R.; Suresh, K.; Valant, M. Structural, magnetic and dielectric properties of rare earth based double perovskites RE2NiMnO6 (RE = La, pr, Sm, Tb). *Physica B: Condensed Matter* **2014**, *448*, 285−289.
(47) Sheikh, M. S.; Ghosh, D.; Dutta, A.; Bhattacharyya, S.; Sinha, T. Lead free double perovskite oxides Ln2NiMnO 6 (Ln = La, Eu, Dy, Lu), a new promising material for photovoltaic application. *Materials Science and Engineering: B* **2017**, *226*, 10−17.
(48) Booth, R.; Fillman, R.; Whitaker, H.; Nag, A.; Tiwari, R.; Ramanujachary, K.; Gopalakrishnan, J.; Lofland, S. An investigation of structural, magnetic and dielectric properties of R2NiMnO6 (R = rare earth, Y). *Mater. Res. Bull.* **2009**, *44*, 1559−1564.
(49) Yang, W. Z.; Liu, X. Q.; Zhao, H. J.; Lin, Y. Q.; Chen, X. M. Structure, magnetic, and dielectric characteristics of Ln2NiMnO6 (Ln = Nd and Sm) ceramics. *J. Appl. Phys.* **2012**, *112*, 064104.
(50) Lekshmi, P. N.; Raji, G. R.; Vasundhara, M.; Varma, M. R.; Pillai, S. S.; Valant, M. Re-entrant spin glass behaviour and magneto-dielectric effect in insulating Sm2NiMnO6 double perovskite. *Journal of Materials Chemistry C* **2013**, *1*, 6565.
(51) Rogado, N. S.; Li, J.; Sleight, A. W.; Subramanian, M. A. Magnetocapacitance and Magnetoresistance Near Room Temperature in a Ferromagnetic Semiconductor: La2NiMnO6. *Adv. Mater.* **2005**, *17*, 2225−2227.
(52) Mukherjee, R.; Ghosh, B.; Saha, S.; Bharti, C.; Sinha, T. Structural and electrical transport properties of a rare earth double perovskite oxide: Ba2ErNbO6. *Journal of Rare Earths* **2014**, *32*, 334−342.
(53) Glazer, A. M. The classification of tilted octahedra in perovskites. *Acta Crystallographica Section B Structural Crystallography and Crystal Chemistry* **1972**, *28*, 3384−3392.
(54) Woodward, P. M. Octahedral Tilting in Perovskites. I. Geometrical Considerations. *Acta Crystallographica Section B Structural Science* **1997**, *53*, 32−43.
(55) Woodward, P. M. Octahedral Tilting in Perovskites. II. Structure Stabilizing Forces. *Acta Crystallographica Section B Structural Science* **1997**, *53*, 44−66.
(56) Halder, S.; Mukherjee, R.; Dutta, A.; Sinha, T. P. Exploring the electronic structure and optical properties of double perovskite Ba2RESbO6 (RE = Ho, Er) from first-principles calculations. *Ferroelectrics* **2017**, *518*, 163−170.
(57) Kangsabanik, J.; Alam, A. Ab Initio Discovery of Stable Double Perovskite Oxides Na2BIO6 (B = Bi, In) with Promising Optoelectronic Properties. *J. Phys. Chem. Lett.* **2020**, *11*, 5148−5155.
(58) Ali, S.; Khan, W.; Murtaza, G.; Yaseen, M.; Ramay, S. M.; Mahmood, A. First principles study of magnetic and electronic properties of A 2 BB′O 6 (A = Ba, Sr) (BB′ = FeRe, MnMo, and MnRe) double perovskites. *J. Magn. Magn. Mater.* **2017**, *441*, 113−123.

https://doi.org/10.1021/acsmaterialsau.2c00031
ACS Mater. Au 2022, 2, 655−664